Stage Separation Dynamics of Spin-Stabilized Rockets

DENNIS R. LONGREN*
Honeywell Inc., Hopkins, Minn.

A method is presented for analyzing the stage separation dynamics of spin stabilized rockets that utilize guide shoes and rails to initially constrain the lateral motion between stages. The derived differential equations describe the angular motions of the upper and lower stages and the forces acting at the guide shoe-guide rail interface. The equations are highly nonlinear and require a high-speed digital computer for effective solution. A typical example shows that coning angles induced during staging can reach magnitudes sufficient to impair the successful operation of upper stages and their experiments.

Nomenclature

F_x,F_y,F_z = summation of forces in body x, y, and z directions, lb
f_1, f_2 = pitch plane guide shoe force on rear, front shoes, lb
g_1,g_2 = yaw plane guide shoe force on rear, front shoes, lb
I_{xx},I_{yy},I_{zz} = roll, pitch, and yaw moments of inertia, slug ft^2
I_{xz} = pitch plane product of inertia, slug ft^2
l_1,l_2 = distance from center of gravity (c.g.) of upper stage to rear, front shoes, respectively, ft
l_3,l_4 = distance from c.g. of lower stage to rear and front guide shoe/guide rail interfaces, respectively, ft
l_5 = distance from lower-stage c.g. to complete vehicle c.g., ft
l_6 = distance from rear shoes to point on upper stage where relative motion is measured, ft
l_7 = distance from lower-stage c.g. to point defined by l_6, ft
L,M,N = summation of moments about body x, y, and z axes, ft-lb
m = mass, slugs
$m_{1,2}$ $\equiv m_1m_2/(m_1 + m_2)$
p,q,r = rotational rates about body x, y, and z axes, rad/sec
t_1 = time when front guide shoes come free, sec
t_2 = time when rear guide shoes come free, sec
u,v,w = components of velocity along body x, y, and z axes, fps
x,y,z = denotes body roll, pitch, and yaw axes in an orthogonal right handed coordinate system with x positive forward
$\Delta\dot{x}$ = relative axial separation velocity between stages, fps
τ = friction force, lb
μ = coefficient of sliding friction between guide shoes and guide rails
$(\dot{})$ = differentiation with respect to time

Subscripts

0, max = initial and maximum values, respectively
1,2 = upper and lower stages, respectively
T = total, or upper plus lower stage

Introduction

PHYSICAL separation of the upper stages of spin stabilized rockets can create unusual dynamic problems that have a major effect on the successful completion of the mission. The problems are aggravated when the upper stage is encased in a payload shield that is attached to the lower stage and protects delicate experiments from exhaust gases, dust, and rain during the flight. This arrangement requires the use of guide shoes and long guide rails to prevent collision between stages during separation. The Scanner and Athena rockets are examples of vehicles that have used this design approach.

The success achieved in employing this staging technique is dependent on the degree of understanding of the separation dynamics. Dwork and Wilke[1,2] provide valuable insight into this problem by developing equations for coning angles based on the conservation of angular momentum. These equations, however, do not provide the degree of detail necessary to evaluate a design or to correlate the observed results from a flight test. The equations developed in this paper provide a complete description of the motion of each stage during the separation event and thus aid in the selection of key design parameters. The need for a rational method of selecting these key design parameters prompted the analysis described in this paper.

Stage separation is initiated with a pressurized bellows, small impulse rockets, or some other device to create an initial relative axial velocity. Guide shoes, sliding on three or four guide rails, effectively keep the stages aligned and help damp the coning motion until only the rear guide shoes remain on the rails. At this time the stages begin acting as though they are joined by a hinge or ball socket joint. Mass imbalance of the spinning rocket will amplify the unstable motion during this phase and may result in pitching or yawing rates reaching 30 deg/sec and tipoff angles reaching 0.26 degrees in only 0.13 sec, as shown later in a typical example using the Scanner configuration. In addition, large forces are created between the guide shoes and rails, and these can cause binding. Collision between the stages after the rear guide shoes leave the rails may also occur as a result of the induced motions.

The failure of a recent Athena flight test was tentatively attributed to excessive hinging motion during staging. This motion apparently resulted in high attitude rates and coning angles after separation, which exceeded the design operating limits of the upper stage attitude controller. This, in turn, probably produced the unsatisfactory performance of the upper stage, which was observed.

The mass imbalance of the lower (or upper) stage is a major factor in the dynamics of separation of spinning stages. This imbalance may easily occur when the lower stage is dynamically balanced by addition of weights after being loaded with propellant. This does not assure dynamic balance after motor burnout, particularly if the motor case was not dynamically balanced prior to loading. For this reason, im-

Received May 16, 1969; revision received November 17, 1969. The author is indebted to K. E. Gaskell for the programing and checkout of these equations on the H-1800 digital computer. This work was supported by the NASA Langley Research Center, under Contract NAS 1-3828. Their contributions to this effort are gratefully acknowledged.

* Presently Program Manager, Honeywell Inc., Ordnance Division. Member AIAA.

balance of the rocket is most likely to occur in the lower or burned out stage.

Since the algebraic sign and magnitude of the imbalance (product of inertia) cannot be determined a priori, it will be assumed to be positive and to lie in the body axis pitch plane. Fixing the imbalance in this manner produces a unique relationship between the body axis rotational rates and the roll angle. This assumption must also be used in the analysis leading to a definition of the initial conditions at the start of staging to maintain consistency with the equations derived herein. Other assumptions essential to a tractable solution of the stage separation problem are:

1) Each stage is symmetrical about the vehicle center line ($I_{yy} = I_{zz}$).

2) The upper stage has no mass imbalance;, therefore, its products of inertia are zero.

3) Spin rates of upper and lower stages are equal and essentially constant over the duration of the analysis.

4) No aerodynamic or reaction forces or moments.

5) No internal rotating machinery with any significant angular momentum.

6) The upper and lower stages are rigid bodies with constant mass, and each has constant moments and products of inertia.

The general analysis approach is to divide the motion into two discrete phases and to use the terminal conditions of phase one as the initial conditions for phase two. The resultant total motion is then the sum of the individual parts.

Relative Motion with All Guide Shoes Attached

This phase is characterized by decreasing relative axial velocity due to guide shoe/rail friction, and by no relative lateral motion between the stages. The phase is assumed to begin immediately after the initial separation velocity has been established by the bellows or rocket motors, and to terminate when the front guide shoes leave the guide rails. The primary variables to be evaluated are the forces acting on the guide shoes, the friction force between the guide shoes and the rails, the reduction of separation velocity produced by this friction force, and the change of vehicle pitch and yaw rates during this phase.

Rotational Motion

The variation of pitch and yaw body attitude rates are treated first and are obtained from a numerical solution of the nonlinear six-degree-of-freedom equations of motion given in Ref. 3.

$$\begin{vmatrix}\dot{u}\\ \dot{v}\\ \dot{w}\end{vmatrix} = \frac{1}{m}\begin{vmatrix}F_x\\ F_y\\ F_z\end{vmatrix} - \begin{vmatrix}o & -r & q\\ r & o & -p\\ -q & p & o\end{vmatrix}\begin{vmatrix}u\\ v\\ w\end{vmatrix} \tag{1}$$

$$\begin{vmatrix}\dot{p}\\ \dot{q}\\ \dot{r}\end{vmatrix} = \begin{vmatrix}I_{xx} & -I_{xy} & -I_{xz}\\ -I_{xy} & I_{yy} & -I_{yz}\\ -I_{xz} & -I_{yz} & I_{zz}\end{vmatrix}^{-1}\left[\begin{vmatrix}L\\ M\\ N\end{vmatrix} - \begin{vmatrix}\dot{I}_{xx} & -\dot{I}_{xy} & -\dot{I}_{xz}\\ -\dot{I}_{xy} & \dot{I}_{yy} & -\dot{I}_{yz}\\ -\dot{I}_{xz} & -\dot{I}_{yz} & \dot{I}_{zz}\end{vmatrix}\begin{vmatrix}p\\ q\\ r\end{vmatrix} - \begin{vmatrix}o & -r & q\\ r & o & -p\\ =q & p & o\end{vmatrix}\begin{vmatrix}I_{xx} & -I_{xy} & -I_{xz}\\ -I_{xy} & I_{yy} & -I_{yz}\\ -I_{xz} & -I_{yz} & I_{zz}\end{vmatrix}\begin{vmatrix}p\\ q\\ r\end{vmatrix}\right] \tag{2}$$

The total vehicle is treated as a rigid body of constant mass with time varying pitch and yaw moments of inertia. This variation of moment of inertia is due only to the increasing over all length of the vehicle as the stages slide apart on the guide rails. The mass and moments of inertia of each stage, by themselves, are constant. The rigid body assumption is merely an extension of the condition of no relative lateral motion between the stages. The resultant pitch and yaw body attitude rates are utilized later in the equations for guide shoe-guide rail interface forces, and also provide essential initial conditions for the next phase of the analysis. Moments of inertia and moment of inertia rates are required for the solution and are calculated as shown. Note that the total pitch moment of inertia rate is nonzero even though the stage mass rates and inertia rates are zero;

$$I_{yyT} = I_{yy1} + m_1(l_1 + l_3 - l_5)^2 + I_{yy2} + m_2 l_5^2 \tag{3}$$

$$m_1(l_1 + l_3 - l_5) = m_2 l_5 \tag{4}$$

combining

$$I_{yyT} = I_{yy1} + I_{yy2} + m_{1,2}(l_1 + l_3)^2 \tag{5}$$

differentiating

$$\dot{I}_{yyT} = 2m_{1,2}(l_1 + l_3)\Delta\dot{x} \tag{6}$$

also

$$I_{xxT} + I_{xx1} + I_{xx2},\ I_{xx2} = I_{xxT} \tag{7}$$

$$l_3 = l_{30} + \int_{t_0}^{t} \Delta\dot{x}dt \tag{8}$$

The general procedure for evaluating the guide shoe forces is to treat each stage as a free body acted upon by forces and moments created by the coning motion and by mass imbalance acting at the guide shoe-guide rail interfaces. The constraint of no relative lateral motion between the stages means that the forces acting at the guide shoe-guide rail interface must be equal and opposite on each stage. In addition, this constraint also requires that the body axis pitch and yaw rotation rates and the lateral translation velocities of each stage be equal. The result is two sets of two simultaneous equations, each set containing the guide shoe-guide rail interface forces. The friction forces and resultant axial velocity reduction are then readily obtainable.

Pitch Plane Forces

For body 1 (upper stage)

$$F_z = f_1 + f_2,\ M = f_1 l_1 + f_2 l_2 \tag{9}$$

For body 2 (lower stage)

$$F_z = -f_1 - f_2,\ M = f_1 l_3 + f_2 l_4 \tag{10}$$

From (1) and (2)

$$\dot{w} = [F_z/m] + qu - pv \tag{11}$$

$$\dot{q} = [1/I_{yy}][M + pr(I_{yy} - I_{xx}) + I_{xz}(r^2 - p^2)] \tag{12}$$

The constraint of no relative lateral motion at either guide shoe requires that

$$\dot{w}_1 = \dot{w}_2,\ u_1 - u_2 \equiv \Delta\dot{x},\ v_1 = v_2 \tag{13}$$

$$\begin{gathered} p_1 = p_2 = p,\ q_1 = q_2 = q \\ \dot{q}_1 = \dot{q}_2,\ r_1 = r_2 = r \end{gathered} \tag{14}$$

Equations (11) and (12) are written for each body using Eqs. (9) and (10) to represent the forces and moments. Use of the relationships of (13) and (14) yield two final equations in two unknowns (f_1 and f_2). One equation represents the constrained balance of forces on each stage, and the other equation represents the constrained balance of moments.

$$f_1 + f_2 = -m_{1,2}q\Delta\dot{x} \tag{15}$$

$$f_1\left(l_1 - \frac{I_{yy1}l_3}{I_{yy2}}\right) + f_2\left(l_2 - \frac{I_{yy1}l_4}{I_{yy2}}\right) = pr\,\frac{(I_{xx1} - I_{yy1}I_{xx2})}{I_{yy2}} - \frac{I_{yy1}I_{xx2}p^2}{I_{yy2}} \tag{16}$$

Yaw Plane Forces

These equations are developed in a manner similar to the pitch plane equations.

For body 1:

$$F_y = g_1 + g_2,\ N = -g_1 l_1 - g_2 l_2 \tag{17}$$

For body 2:

$$F_y = -g_1 - g_2,\ N = -g_1 l_3 - g_2 l_4 \tag{18}$$

$$\dot{v} = [F_y/m] + pw - ru \tag{19}$$

$$\dot{r} = [1/I_{yy}][N + pq(I_{xx} - I_{yy}) + I_{xz}(\dot{p} - qr)] \tag{20}$$

The $\dot{p}$ term cannot be disregarded even though p is assumed constant over the short duration of the analysis; however, it can generally be assumed that $p^2 \gg r^2$ without significant error. The expression for $\dot{p}$ is

$$\dot{p} = [1/I_{xx}][L + I_{xz}(pq + \dot{r})] \tag{21}$$

In addition to the relationships of (13) and (14), the constraint of no lateral motion at either guide shoe in either plane requires that

$$w_1 = w_2,\ \dot{v}_1 = \dot{v}_2,\ \dot{r}_1 = \dot{r}_2 \tag{22}$$

Combining

$$g_1 + g_2 = m_{1,2} r \Delta\dot{x} \tag{23}$$

$$g_1\left(l_1 - \frac{l_3 I_{yy1} I_{xz2}}{I_{xx2} I_{yy2} - I_{xz2}^2}\right) + g_2\left(l_2 - \frac{l_4 I_{yy1} I_{xz2}}{I_{xx2} I_{yy2} - I_{xz2}^2}\right) = \frac{I_{yy1} I_{xz2} I_{xz2} qr}{I_{xx2} I_{yy2} - I_{xz2}^2} + pq\left[I_{xx1} - I_{yy1} - \frac{I_{yy1} I_{xx2} I_{yy2}}{I_{xx2} I_{yy2} - I_{xz2}^2} \times \left(\frac{I_{xx2}}{I_{yy2}} + \frac{I_{xz2}^2}{I_{xx2} I_{yy2}} - 1\right)\right] \tag{24}$$

where

$$l_4 = l_{4_0} + \int_{t_0}^{t} \Delta\dot{x}\, dt. \tag{25}$$

The solution of Eqs. (15, 16, 23, and 24) requires knowledge of the body axis attitude rates q and r as functions of time. These are obtained from Eqs. (1) and (2) which include the effects of the lower stage mass imbalance and variable inertia. The initial conditions for use in those equations are obtained from a separate six-degree-of-freedom simulation of the rocket from launch to beginning of staging. Solution of Eqs. (1) and (2) may be accomplished using standard numerical integration techniques and is not discussed here.

Friction Force and Separation Velocity Decrease

Assuming that sliding friction is proportional to the magnitude of the normal force between the guide shoes and guide rails,

$$\tau = -\mu(|f_1| + |f_2| + |g_1| + |g_2|) \tag{26}$$

and

$$\Delta\dot{x} = \Delta\dot{x}_0 - \left(\int_{t_0}^{t} \tau dt \Big/ m_{1,2}\right) \tag{27}$$

The guide shoe forces vary in a cyclic manner at a frequency equal to the spin rate p. It can be shown that $[f_1^2 + f_2^2 + g_1^2 + g_2^2]^{1/2}$ is a constant at any time regardless of the values of q and r as long as $(q^2 + r^2)^{1/2}$ is constant. It can also be shown through use of Lagrangian multipliers that the maximum friction force is

$$\tau_{\max} = -2\mu(f_1^2 + f_2^2 + g_1^2 + g_2^2)^{1/2} \tag{28}$$

During the staging event, this maximum force occurs only when

$$|f_1| = |f_2| = |g_1| = |g_2| \tag{29}$$

This rather elementary analysis of the friction force conforms with the original assumption of the upper and lower stages being rigid bodies. This is a good assumption for the Scanner and Athena rockets; however, a more detailed analysis may be required if the effects of elasticity or structural oscillations are felt to be important.

Relative Motion with Only Rear Guide Shoes Attached

This phase begins when the front guide shoes come free and is characterized by a further decrease in axial separation velocity and no relative lateral motion at the rear guide shoes. The stages are permitted to rotate in pitch and yaw relative to each other with the rear guide shoes acting as a pivot. The stages react, in effect, as though they are joined by a ball and socket joint.

The primary variables to be studied are the degree of pitching and yawing motion of each stage, the relative angular motion between stages, the normal force on the rear guide shoes, the tipoff moment, and the reduction of separation velocity due to friction.

The general procedure is to treat each stage as a free body acted upon by the rear guide shoe-guide rail interface forces. Equations of motion are written for the balance of forces and moments in the pitch and yaw planes. Applying the constraint of no relative lateral motion at the guide shoe/rail interface in either plane yields four simultaneous nonlinear differential equations that describe the pitching and yawing motion during this phase. In addition, two equations describing the pitch and yaw plane guide shoe forces are obtained. The relative motion is obtained after integrating the relative velocity between stages at any point of interest. The reduction of separation velocity is obtained by integrating the effect of the guide shoe friction forces as described previously.

Guide Shoe Forces

There can be no relative motion between stages in the pitch or yaw planes at the rear guide shoes. Thus

$$q_1 l_1 + w_1 = -q_2 l_3 + w_2 \tag{30}$$

$$-r_1 l_1 + v_1 = r_2 l_3 + v_2 \tag{31}$$

Differentiating,

$$l_1 \dot{q}_1 + \dot{w}_1 = -q_2 \dot{l}_3 - l_3 \dot{q}_2 + \dot{w}_2 \tag{32}$$

$$-l_1 \dot{r}_1 + \dot{v}_1 = r_2 \dot{l}_3 + l_3 \dot{r}_2 + \dot{v}_2 \tag{33}$$

where

$$\dot{l}_3 = \Delta\dot{x} = u_1 - u_2 \tag{34}$$

From Eq. (1)

$$\dot{w}_1 = [f_1/m_1] + q_1 u_1 - p v_1 \tag{35}$$

$$\dot{w}_2 = -[f_1/m_2] + q_2 u_2 - p v_2 \tag{36}$$

$$\dot{v}_1 = [g_1/m_1] + p w_1 - r_1 u_1 \tag{37}$$

$$\dot{v}_2 = -[g_1/m_2] + p w_2 - r_2 u_2 \tag{38}$$

Combining Eqs. (31, 32, and 34–36) yields

$$f_1 = m_{1,2}[u_1(q_2 - q_1) + l_1(pr_1 - \dot{q}_1) + l_3(pr_2 - \dot{q}_2) - 2q_2\Delta\dot{x}] \tag{39}$$

Equations (30, 33, 34, 37, and 38) yield

$$g_1 = m_{1,2}[u_1(r_1 - r_2) + l_1(\dot{r}_1 + pq_1) + l_3(\dot{r}_2 + pq_2) + 2r_2\Delta\dot{x}] \tag{40}$$

Equations (39) and (40) provide the pitch and yaw plane guide shoe forces; l_3 is defined by Eq. (8).

Rotational Motion

From Eq. (2),

$$\dot{q}_1 = [f_1 l_1 + pr_1(I_{yy1} - I_{xx1})]/I_{yy1} \quad (41)$$

$$\dot{q}_2 = [f_1 l_3 + pr_2(I_{yy2} - I_{xx2}) - I_{xz2}p^2]/I_{yy2} \quad (42)$$

$$\dot{r}_1 = [-g_1 l_1 + pq_1(I_{xx1} - I_{yy1})]/I_{yy1} \quad (43)$$

$$\dot{r}_2 = [-g_1 l_3 + pq_2(I_{xx2} - I_{yy2}) + I_{xz2}(\dot{p}_2 - q_2 r_2)]/I_{yy2} \quad (44)$$

From Eq. (21)

$$\dot{p}_2 = [L_2 + I_{xz2}(pq_2 + \dot{r}_2)]/I_{xx2} \quad (45)$$

and

$$L_2 = -L_1 = -I_{xx1}\dot{p}_1, \text{ since } I_{xz1} = 0 \quad (46)$$

$$\therefore \dot{p}_2 = [I_{xz2}/I_{xxT}](pq_2 + \dot{r}_2) \quad (47)$$

Incorporating Eqs. (39, 40, and 47) into Eqs. (41–44) yields:

$$\dot{q}_1 = K_1 r_1 + K_2[u_1(q_2 - q_1) + l_3(pr_2 - \dot{q}_2) - 2q_2\Delta\dot{x}] \quad (48)$$

$$\dot{q}_2 = \frac{1}{[1 + K_3 l_3^2(1 - K_2 l_1)]}\left\{pr_2(K_4 + K_3 l_3^2) + K_3 l_3 \times [u_1(q_2 - q_1)(1 - K_2 l_1) + l_1 r_1(p - K_1) - K_2 l_1 l_3 pr_2 + 2q_2\Delta\dot{x}(K_2 l_1 - 1)] - \frac{I_{xz2}p^2}{I_{yy2}}\right\} \quad (49)$$

$$\dot{r}_1 = -K_1 q_1 - K_2[u_1(r_1 - r_2) + l_3(pq_2 + \dot{r}_2) + 2r_2\Delta\dot{x}] \quad (50)$$

$$\dot{r}_2 = \frac{-1}{\left[1 + K_3 l_3^2(1 - K_2 l_1) - \frac{I_{xz2}^2}{I_{yy2}I_{xxT}}\right]}\left\{pq_2(K_4 + K_3 l_3^2) + K_3 l_3[u_1(r_1 - r_2)(1 - K_2 l_1) + l_1 q_1(p - K_1) - K_2 l_3 l_1 pq_2 + 2r_2\Delta\dot{x}(1 - K_2 l_1)] - \frac{I_{xz2}}{I_{yy2}}q_2\left[\frac{I_{xz2}}{I_{xxT}}p - r_2\right]\right\} \quad (51)$$

where

$$K_1 = \frac{p[(1 - I_{xx1}/I_{yy1}) + (l_1^2/I_{yy1})(m_{1,2})]}{1 + l_1^2 m_{1,2}/I_{yy1}} \quad (52)$$

$$K_2 = \frac{l_1 m_{1,2}/I_{yy1}}{1 + l_1^2 m_{1,2}/I_{yy1}} \quad (53)$$

$$K_3 = m_{1,2}/I_{yy2}, \quad K_4 = 1 - [I_{xz2}/I_{yy2}] \quad (54)$$

The accelerations $\dot{q}_1$, $\dot{q}_2$, $\dot{r}_1$, and $\dot{r}_2$ change instantaneously when the front guide shoes come free and again when the rear shoes come free; however, the attitude rates q_1, q_2, r_1, and r_2 are continuous across these discontinuities. Therefore, the attitude rates existing when the front guide shoes come free form the initial conditions for integration of Eqs. (48–51). These equations are solved by using standard numerical integration techniques to provide the attitude rate time history for this phase of the analysis.

Table 1 Scanner spacecraft physical data

I_{xx1} = 9.22 slug ft²	l_{3_0} = 9.63 ft
I_{xx2} = 22.73 slug ft²	l_{4_0} = 12.17 ft
I_{yy1} = 193.8 slug ft²	m_1 = 28.53 slugs
I_{yy2} = 1344.0 slug ft²	m_2 = 26.05 slugs
I_{xz1} = 0	p_0 = 29.8 rad/sec
l_{xz2} = 3.4 slug ft²	u_1 = 7433 fps
l_1 = 2.966 ft	$\Delta\dot{x}_3$ = 20.0 fps
l_2 = 0.425 ft	μ = 0.1

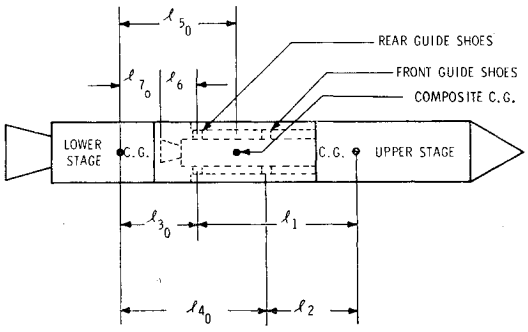

Fig. 1 Definition of physical dimensions.

Relative Motion between Stages

The relative lateral velocity between stages in the pitch plane at any point defined by l_6 is

$$W = q_1(l_1 + l_6) + w_1 - (-q_2 l_7 + w_2) \quad (55)$$

Combining this with Eq. (30), we have

$$W = l_6(q_1 - q_2) \quad (56)$$

Similarly, in the yaw plane

$$V = l_6(r_2 - r_1) \quad (57)$$

where q_1, q_2, r_1, and r_2 are obtained from an integration of Eqs. (48–51).

The relative motion in each plane is obtained by integrating the relative velocity components. Total relative motion is obtained from:

$$R = \left\{\left[\int_{t_1}^{t_2} V dt\right]^2 + \left[\int_{t_1}^{t_2} W dt\right]^2\right\}^{1/2} \quad (58)$$

$$\text{relative angle} = \sin^{-1} R/l_6 \quad (59)$$

From a study of Ref. 4 we find

$$\text{coning angle} = \tan^{-1}\frac{I_{yy1}}{I_{xx1}}\frac{(q_1^2 + r_1^2)^{1/2}}{p} \quad (60)$$

and

$$\text{tipoff moment} = l_1(f_1^2 + g_1^2)^{1/2} \quad (61)$$

where f_1 and g_1 are obtained from Eqs. (39) and (40).

The friction force between guide shoes and rails and the resultant velocity decrease are evaluated using Eqs. (26) and (27) with f_2 and g_2 set to zero. Again it can be shown through use of Lagrangian multipliers that the maximum friction force is

$$\tau_{\max} = -1.414\mu(f_1^2 + g_1^2)^{1/2} \quad (62)$$

which occurs only when $|f_1| = |g_1|$.

The motion of the upper and lower stages after the rear guide shoes are free is computed, if desired, by applying Eqs. (1) and (2) to each body independently and using the results of Eqs. (48–51) at $t = t_2$ as initial conditions. Relative motion may then be obtained by differencing the appropriate parameters.

Illustrative Example

The general motion observed during Athena and Scanner flight tests conform with the results predicted. However, telemetered information on the detailed dynamic motion occurring during flight is meager, and no attempt has been made to reconstruct the observed results using the equations derived herein. But derived equations were applied during a design analysis of the stage separation characteristics of an earlier version of the Scanner spacecraft. The essential physical data and calculated coefficients are given in Table 1. Figure 1 illustrates the relationship between some of the parameters.

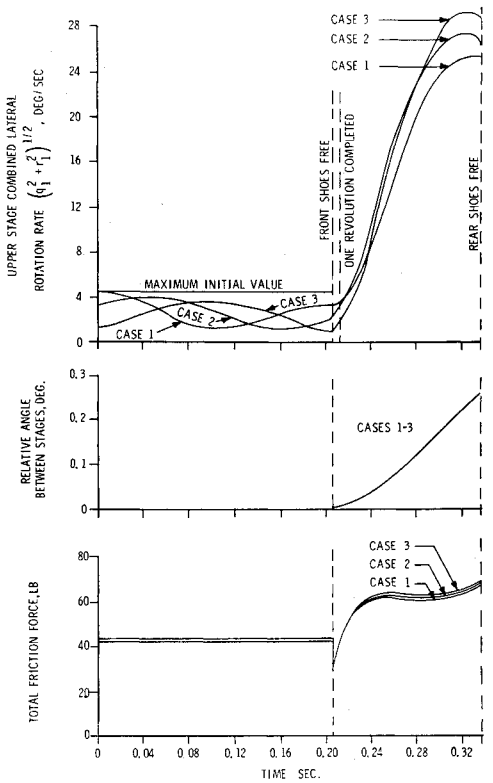

Fig. 2 (Top) Angular rates of rotation. (Center) Relative angle between centerlines of upper and lower stages. (Bottom) Friction force between guide shoes and rails.

A dynamic simulation of the complete launch vehicle from liftoff to the beginning of the staging event was conducted by the Langley Research Center. The mass imbalance of the booster was assumed to lie in the pitch plane. This resulted in a unique combination of pitching and yawing rates as functions of time. It was found that any combination of rates satisfying Eq. (63) could occur at the beginning of the staging event.

$$q_0^2 + (r_0 - 0.0285)^2 = 24.5 \times 10^{-4} \qquad (63)$$

Three specific examples were selected for numerical evaluation and are designated as cases 1–3. For case 1, q_0 (rad/sec) = 0 and r_0 (rad/sec) = 0.078; for case 2, $q_0 = -0.0495$ and $r_0 = 0.0285$; for case 3, $q_0 = 0$ and $r_0 = -0.021$.

Equations 1, 2, and 48–51 were solved and combined to provide the total upper stage lateral rotation rate $(q_1^2 + r_1^2)^{1/2}$ history shown in Fig. 2. Due to the rapidly increasing pitch and yaw moments of inertia of the combined stages as they separate, this combined rotation rate decays in a cyclic manner until the front guide shoes come free. The rotation rates build very rapidly after the front guide shoes come free. During this phase the effect of the ball and socket joint between the stages is quite apparent, as peak rotation rates of near 30°/sec are attained. After separation, the spacecraft will retain this rate in the form of free coning motion. These high rates have been shown to be produced almost entirely by the product of inertia of the lower stage which acts as a forcing function through the rear guide shoes. The effects of the different possible combinations of initial body attitude rates and small expected variations of vehicle mass parameters have little effect on the general characteristics of this motion. The rotation rates attained are high enough to have a major influence on any attitude stabilization system installed in the spacecraft.

The distance between the front and rear guide shoes in this case is such that the vehicle rolls through about 180° in the time interval between release of the front and rear shoes. Repositioning either or both of these shoes so that the distance between them is about twice the present value would permit the body rates to return to acceptably low values at the time the rear shoes come free, thus minimizing the free coning motion of the spacecraft after separation. However, the large possible variation of spin rates produces a similar variation in the time required to roll through one revolution. Therefore, the distance between the guide shoes could effectively be "tuned" for only one spin rate, and unacceptably high lateral body rates could still occur if the spin rate deviates from the normal value.

The relative angle between the centerlines of the upper and lower stages reaches a peak of 0.26° when the rear guide shoes come free, as shown in Fig. 2. The rapid build-up of this angle attests to the need for separating the stages in the shortest possible time. The various combinations of initial pitch and yaw rates have some effect on the final relative angle, but the differences are quite small.

The frictional force between the guide shoes and rails was determined and is shown in Fig. 2. The forces on the rear shoes change instantaneously when the front shoes come free, as shown. The friction force is large enough to produce a 6% decrease in separation velocity during the event. It is conceivable, however, that the interstage guide shoe forces could become large enough to produce binding between the shoes and rails under more extreme conditions.

References

[1] Dwork, M., "Coning Effects Caused by Separation of Spin-Stabilized Stages," *AIAA Journal*, Vol. 1, No. 11, Nov. 1963, pp. 2639–2640.

[2] Wilke, R. O., "Comment on 'Coning Effects Caused by Separation of Spin-Stabilized Stages'," *AIAA Journal*, Vol. 2, No. 7, July 1964, p. 1358.

[3] Brown, R. C. et al., "Six-Degree-of-Freedom Flight-Path Study Generalized Computer Program," Pt 1, WADD TR 60-781, May 1961, Flight Dynamics Lab., Wright-Patterson Air Force Base, Dayton, Ohio.

[4] Martz, C. W., "Method for Approximating the Vacuum Motions of Spinning Symmetrical Bodies with Non Constant Spin Rates," R-115, 1961, NASA.

Bibliography

Binion, T. W., Jr. and Herron, R. D., "Pressure and Forces on a Missile Model Resulting from Stage Separation at Very High Altitude," TDR 62-195, Nov. 1962, Arnold Engineering Development Center, Tullahoma, Tenn.

Wasko, R. A., "Experimental Investigation of Stage Separation Aerodynamics," TN D-868, May 1961, NASA.

Smoot, L. D., "Prediction of Interstage Pressure in Multistage Solid-Propellant Rocket Systems," *AIAA Journal*, Vol. 1, No. 10, Oct. 1963, p. 2361.

Jarmolow, K., "Dynamics of a Spinning Rocket with Varying Inertia and Applied Moment," *Journal of Applied Physics*, Vol. 28, No. 3, March 1957, pp. 308–313.

Lundstrom, R. R., Henning, A. B., and Hook, W. R., "Description and Performance of Three Trailblazer II Re-entry Research Vehicles," TN D-1866, Dec. 1964, NASA.

Buglia, J. J. et al., "Analytical Method of Approximating the Motion of a Spinning Vehicle with Variable Mass and Inertia Properties Acted Upon by Several Disturbing Parameters," R-110, 1961, NASA.

Young, G. R. and Buglia, J. J., "An Analysis of the Coning Motions of the Final Stages of Three NASA Scout De-

velopment Vehicles," TN D-1396, Dec. 1962, NASA.
Barnes, D. R., "Analysis of Dynamics of Mother-Daughter Rocket Separation Systems," NASA CR 55153, 1963, Penn State Univ. Ionosphere Research Lab., University Park, Penn.
Abbot, H. M., "Bibliography-Separation and Ejection Systems of Flight Vehicles," SB 64-14, July 1964, Lockheed Missiles & Space Co., Sunnyvale, Calif.
Narahara, R. M., "Computer-Aided Design," *Space/Aeronautics*, Vol. 52, No. 7, Dec. 1969, pp. 56–58.

APRIL 1970 J. SPACECRAFT VOL. 7, NO. 4

Computer Analysis of Complex Shell Structures

DAVID BUSHNELL*
Lockheed Palo Alto Research Laboratory, Palo Alto, Calif.

A digital computer program for the general analysis of composite ring-stiffened shells of revolution is used for the analysis of two typical liquid-propellant rocket nozzle configurations. The program, called BOSOR3, is briefly described. It is then shown how the mathematical models of the nozzles are constructed. These nozzles are of complex wall construction and are submitted to internal pressure, axial compression, and bending. In the analysis the nozzles are treated as segmented, longitudinally stiffened, orthotropic layered shells. A stress analysis and a stability analysis are performed for each of the two nozzle configurations. Comparisons with the test results are given. The predicted failure load and mode agree well with those observed in the test. It is determined that both nozzle configurations are stress-critical, failure of the wall material first occurring just aft of the throat in the outer fibers of the wall.

Nomenclature

A = cross section area, in.^{2}
e_1,e_2 = radial, axial distances from reference surface (coolant pipe centerline) to discrete ring centroid, in.
E = Young's modulus, psi
G = shear modulus, psi
I = moment of inertia, in.^{4}
J = torsion constant, in.^{4}
L = distance from point of application of lateral load S to end B of nozzle (Fig. 2)
$\bar{M}$ = effective moment at nozzle throat ($\bar{M} = 51S$), in.-lb
M_{10} = meridional moment resultant, positive for compressive stress in outer fiber at $\theta = 0$, in.-lb/in.
N_{10},N_{20} = meridional, circumferential stress resultants, positive for tension, lb/in.
n = number of circumferential waves
p = chamber pressure, psi
Q = transverse applied shear load/length, lb/in.
r = radius from centerline to reference surface, measured normal to axis of revolution, in.
S = lateral load (Fig. 2), lb
s = arc length measured from clamped end A
t = thickness, in.
$T(2)$ = distance from centroid of coolant pipes to wire windings, in.
T = axial thrust, positive compression, lb
u,v,w = meridional, circumferential, normal displacement components, in.
V = axial load/length, lb/in.
x,y = axes attached to discrete rings (Fig. 4b)
z = axial distance along nozzle, in.
λ = Lagrange multiplier
θ = circumferential coordinate
χ = rotation of meridian in its plane
ν = Poisson's ratio

Subscripts

B = value at end B of nozzle (Fig. 2)
i = mesh point number
p = pertaining to coolant pipes
t = value at nozzle throat
0 = prebuckling quantity
1,2 = meridional and circumferential directions, respectively
12 = twist or shear

Received January 30, 1969; revision received November 19, 1969. This research was sponsored by the Aerojet-General Corporation, Sacramento, Calif.

* Staff Scientist, Aerospace Sciences Laboratory. Member AIAA.

Introduction

Tests on Liquid-Propellant Nozzles

FIGURE 1 shows a nozzle for a liquid-propellant rocket that was tested under combined static loads at the Aerojet-General Corporation in Sacramento, Calif.[1] The nozzle consists of steel coolant pipes which run in the meridional direction. These pipes form a layer of the nozzle wall, which is reinforced by steel wire wound circumferentially over portions of the surface and by a number of discrete ring stiffeners. The test nozzle with applied loads is sketched in Fig. 2. It is clamped at A and bolted to a cylinder at B. The cylinder is free to translate and rotate as a rigid body. The static lateral load S simulates a transient bending moment caused primarily by forces imposed upon the nozzle by the inertia of its aft skirt during ignition and initial firing of the engine.

Three tests were performed on the nozzle shown in Fig. 1. In the first test the chamber was pressurized to 700 psi and a maximum compressive thrust load $T = 10{,}230$ lb was applied in increments and then removed. A maximum shear load $S = 1000$ lb was then applied in increments and removed, after which the chamber was returned to zero pressure. The coolant pipes were pressurized to 1000 psi throughout this test. No damage was sustained by the nozzle. In the second test brittle lacquer (Stresscoat) was applied to the exterior throat. After the coolant pipes and the chamber had been pressurized to 1000 and 700 psi, respectively, a maximum thrust load of 43,000 lb was applied in increments and held. An indicated shear load of 1200 lb was then applied in increments. The loads and pressures were removed and the chamber inspected. The actual applied shear load, corrected for pin friction and side component of thrust, amounted to about 1000 lb during this run. There was no apparent damage. In the third test the loading sequence was the same